Macromolecules 1984, 17, 2674-2678

Rotational Isomeric State Calculations of the Dynamic Structure Factor and Related Properties of Some Linear Chains. 2. First Cumulant of the Dynamic Structure Factor

Kanji Kajiwara[†] **and Walther Burchard***[‡]

Institute for Chemical Research, Kyoto University, Uji, Kyoto-fu, 611 Japan,
and Institut für Makromolekulare Chemie der Universität Freiburg,
7800 Freiburg i. Brsg., West Germany. *Received March 16, 1984*

ABSTRACT: The particle scattering factor and the first cumulant of the dynamic structure factor of poly(methylene), poly(oxymethylene), *cis*-1,4-polybutadiene, and *trans*-1,4-polybutadiene were calculated by the same technique as outlined in part 1. For $q > 0.2$ nm^{-1}, which corresponds to a length of the subchain of $r_{ij} < 0.8$ nm, the influence of directional correlation due to chain stiffness or rotational hindrance becomes effective and causes the expected deviations from the Gaussian behavior. As expected, no general form for the asymptote of Γ in this far-q region was obtained for the nondraining limit. This region is defined by the special characteristics of the microstructure of the individual chains. When the free-draining contribution is taken into account, the reduced first cumulant Γ/q^2 in a certain region increases linearly with q. The proportionality coefficient increases slightly with the characteristic ratio C_∞, i.e., with chain stiffness, and is in every case larger than that of a Gaussian chain. This coefficient in the asymptotic region of large q is related to the coefficient C in $\Gamma/q^2 = D(1 + C\langle S^2\rangle q^2 - ...)$ of the reduced first cumulant at small q values and again for the simulated chains is larger than for the Gaussian chain.

Introduction

In the preceding paper, part 1,[1] of this study we reported rotational isomeric state (RIS) calculations of the geometric and hydrodynamic radii and of the related ρ parameters for a number of realistic chain molecules. A slight increase of the ρ parameter with the characteristic ratio C_∞, i.e., chain stiffness, was found and discussed. The present paper now deals with the particle scattering factor $P(q)$ and the angular dependence of the first cumulant Γ of the dynamic structure factor $S(q,t)$ for the same chains as those treated in part 1. Again the RIS model has been chosen as the basis of the calculations.

According to Akcasu and Gurol,[2] the first cumulant of the dynamic structure factor is given in terms of equilibrium averages as follows:

$$\Gamma = \sum_j\sum_k\langle(\mathbf{q}\cdot\mathbf{D}_{jk}\cdot\mathbf{q})\exp(i\mathbf{q}\cdot\mathbf{r}_{jk})\rangle_{\mathrm{eq}}\Big/\sum_j\sum_k\langle\exp(i\mathbf{q}\cdot\mathbf{r}_{jk})\rangle_{\mathrm{eq}} \quad (1)$$

where the angular brackets denote the average over the equilibrium distance distribution between the two chain elements j and k. $\mathbf{D}_{jk}$ is the element of the diffusion tensor for this pair of chain elements and is given by

$$\mathbf{D}_{jk}/k_{\mathrm{B}}T = \delta_{jk}\zeta_j^{-1}\mathbf{1} + (1 - \delta_{jk})(8\pi\eta_0\mathbf{r}_{jk})^{-1}(1 + \mathbf{r}_{jk}\mathbf{r}_{jk}/r_{jk}^2) \quad (2)$$

Here, $\mathbf{r}_{jk}$ is the vector from the jth to the kth element, η_0 the solvent viscosity, and ζ_j the frictional coefficient of the jth element. The first term results from the friction of the individual bead, while the second term takes account of the hydrodynamic interaction which the kth chain element in the chain exerts on the jth element. Equation 1 implies that the total hydrodynamic interaction in the chain can be approximated by the sum over all chain element pairs $j \neq k$. The denominator in eq 1 is identified as the static structure factor $S(q) = N^2P(q)$, where $P(q)$ is the particle scattering factor.

The averaging procedure may be carried out in two steps. When the vector $\mathbf{r}_{jk}$ is averaged over all orientations, then the scattering function for a pair of chain elements is converted into[2,3]

$$\langle\exp(i\mathbf{q}\cdot\mathbf{r}_{jk})\rangle_{\mathrm{or}} = z^{-1}\sin z \quad (3)$$

$$\langle(\mathbf{q}\cdot\mathbf{D}_{jk}\cdot\mathbf{q})\exp(i\mathbf{q}\cdot\mathbf{r}_{jk})\rangle = q^2k_{\mathrm{B}}T[\delta_{jk}/\zeta_j + \{(1 - \delta_{jk})/(4\pi\eta_0\mathbf{r}_{jk})\}(z^{-1}\sin z + z^{-2}\cos z - z^{-3}\sin z)] \quad (4)$$

with

$$z = qr_{jk} \quad (5)$$

In the second step the averaging is performed over all distances r_{jk}. For linear Gaussian chains an analytical expression can be obtained. Neglecting the free-draining term and replacing the double sum of the nondraining part by an integral, eq 1 with eq 3 yields in the nondraining limit

$$\Gamma/q^2 = (3q^2uA/4N^{1/2}) \times [u + D(u) + 2(u^2 - 1)G(u)]/[u^2 - 1 + \exp(-u^2)] \quad (6)$$

where

$$u^2 = q^2\langle S^2\rangle \quad (7)$$

$$G(u) = \int_0^u x^{-1}D(x)\,\mathrm{d}x \quad (8)$$

$$D(x) = \exp(-x^2)\int_0^x \exp(t^2)\,\mathrm{d}t \quad (9)$$

$$A = k_{\mathrm{B}}T/(6^{1/2}\pi^{3/2}b\eta_0) \quad (10)$$

with $\langle S^2\rangle$ being the mean square radius of gyration and b the effective bond length.

The first cumulant of eq 6 has a characteristic asymptote at large q

$$(\Gamma/q^2) \rightarrow (k_{\mathrm{B}}T/16\eta_0)q \quad (11)$$

which is independent of the chain length, or the mean square radius of gyration, and independent of polymer polydispersity. The result of eq 11 is, however, limited to Gaussian chain statistics and to $qb > 1$ but is valid for any type of polymer architecture, i.e., cyclization or branching.

The region of small and intermediate q values depends significantly, of course, on the polymer architecture. For small q, i.e., $q^2\langle S^2\rangle \ll 1$, the reduced first cumulant follows the relationship[3,4]

$$\Gamma/q^2 = D(1 + Cq^2\langle S^2\rangle - ...) \quad (12)$$

[†] Institute for Chemical Research, Kyoto University.

[‡] Institut für Makromolekulare Chemie der Universität Freiburg.

0024-9297/84/2217-2674$01.50/0

where C is a dimensionless coefficient which differs in a characteristic fashion for branched and cyclic chains as compared to linear ones. It also depends on polydispersity. C can in most cases be calculated analytically.

In the intermediate region of $q^2\langle S^2\rangle \simeq 1$ analytical solutions have been possible so far for linear chains only. For more complex structures a hydrodynamic preaveraging has been applied where the correct scattering pair function is approximated by the following expression:

$$\langle(\mathbf{q}\cdot\mathbf{D}_{jk}\cdot\mathbf{q})\exp(i\mathbf{q}\cdot\mathbf{r}_{jk})\rangle \simeq \langle\mathbf{q}\cdot\mathbf{D}_{jk}\cdot\mathbf{q}\rangle\langle\exp(i\mathbf{q}\cdot\mathbf{r}_{jk})\rangle \quad (13)$$

The error introduced by this preaveraging is small for the linear chain (~15%) but can amount to 40% in a certain q region for highly branched chains. A semiempirical approximation has been suggested[3] to correct the hydrodynamic preaverage approximation, which reduces the error to about 1%. This approximation is still limited to Gaussian chains.

Recently, Schmidt and Stockmayer have carried out calculations of the coefficient C for wormlike stiff chains,[5] where at first a significant increase of C with increasing chain stiffness is observed, but finally a drop to $C = {}^1/_{18}$ of the infinitely thin rod occurs.[5,6] Nothing is known as to whether the microstructure of a realistic chain influences C or the properties of the reduced first cumulant Γ/q^2, particularly in the asymptote of large q. We thus carried out computer simulations on the basis of the RIS model[7] for the same chains as those chosen in part 1, where hydrodynamic preaveraging is not needed.

Simulation Model

The principles of this model simulation have already been discussed in part 1. Here we stress only the essential points of the underlying assumptions and additional details for the calculation of the static and dynamic scattering functions occurring in Γ (the denominator and numerator in eq 1, respectively). Although we avoid the Gaussian chain approximation we still assume the distance between two elements in a chain be independent of the position of the subchain; i.e., the distance is a sole function of the contour length of the subchain.[8] This assumption holds when long-range interactions, i.e., the excluded volume effect, are ignored.

To derive the numerator in eq 1 and likewise the denominator, we have to carry out the averaging over all orientations and all distances between the two elements of a pair, and the result has then to be summed over all N^2 pairs in the molecule. The average for a pair of scattering elements over all orientations can be performed analytically and has already been given in eq 4. The averaging over all interstitial distances and the final summation have to be done numerically. For the most efficient computation we interchanged the last two steps, the averaging procedure and the summation. A chain is first generated by the procedure described in part 1. In this chain all distances r_{jk} are fixed, and therefore $z = qr_{jk}$ can be calculated. Then the summation is carried out, for convenience, by replacing the double sum by a single sum.

$$\sum_j\sum_k z^{-1}\sin z = N + 2\sum_{m=1}^{N-1}(N-m)z^{-1}\sin z \quad (14)$$

$$\sum_j\sum_k(\mathbf{q}\cdot\mathbf{D}_{jk}\cdot\mathbf{q})\exp(i\mathbf{q}\cdot\mathbf{r}_{jk}) = q^2k_BT[\sum_{m=1}^{N}(1/\zeta_m) + (1/2\pi\eta_0)\sum_{m=1}^{N-1}\{(N-m)/r_{1m}\}(z^{-1}\sin z + z^{-2}\cos z - z^{-3}\sin z)] \quad (15)$$

with $z = qr_{1m}$, where r_{1m} denotes the distance between the first and the mth element. Then another chain is generated and the summation performed in the same manner. The result for each q value for the various chains is subsequently summed and divided by the number of generated chains, which yields the required ensemble average; 5000 chains were generated for each of the chosen realistic molecules. Since the shape of the particle scattering factors and of the first cumulants is rather insensitive to the number of chain elements N in the range $q > 1$ nm^{-1}, we fixed $N = 400$ for each polymer in the present simulation.

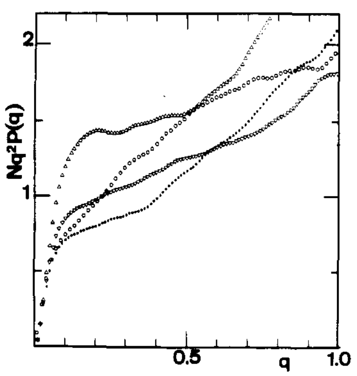

Figure 1. Kratky plots for the particle scattering factors of poly(methylene) (○), poly(oxymethylene) (●), *cis*-1,4-polybutadiene (△), and *trans*-1,4-polybutadiene (▽).

Results and Discussion

Particle Scattering Factor. The particle scattering factor for small $q^2\langle S^2\rangle$ is fully determined by the mean square radius of gyration and in this region shows no difference for the various polymers when plotted against $q^2\langle S^2\rangle = u^2$. Differences in the shape become observable at larger u^2 and in particular in the asymptotic region of $u^2 \gg 1$. An appropriate means of studying the asymptotic region is the Kratky plot, where $q^2P(q)$ is plotted against q. For Gaussian chains the particle scattering factor in this plot approaches a plateau, whereas a thin rodlike molecule exhibits a straight line with a positive slope. Because of the hindrance to internal rotation, every realistic chain will generate a specific microstructure which, in many cases, can be approximated by a rod extending over a certain length, which is called the persistence length. According to Porod and Kratky the change (now usually called the "crossover") from the Gaussian to the rodlike behavior should occur at $qa = 1.91$,[9,10] where a is the persistence length, which for the flexible chains of the present consideration is on the order of 1 nm.

Figure 1 shows the Kratky plots for the simulated poly(methylene), poly(oxymethylene), and *cis*-1,4- and *trans*-1,4-polybutadienes. Zierenberg et al.[8] have employed the same method to estimate the particle scattering factor for poly(methylene), and their result is consistent with the present findings. Deviations from the Gaussian chain behavior are observed in all cases when q exceeds 0.2 nm^{-1}, which is by a factor 5 earlier than expected from Porod's estimation. Similar deviations have been found also for the idealized wormlike chain, where the crossover never appears as a kink point but is actually a broader region which starts already at much lower q values.

The scattering behavior at large $q > 1$ nm^{-1} is expected to show the rodlike behavior for the wormlike chain but will show special characteristics for realistic chains as result of their individual microstructure. A wobbled helix, for instance, as realized by poly(oxymethylene), will show different behavior from that of a *cis*-1,4-polybutadiene chain. Hence no general asymptotic behavior can be expected in accordance with the present findings. Recently,

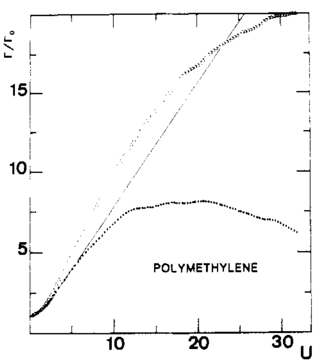

Figure 2. Normalized apparent diffusion coefficient Γ/Γ_0 of poly(methylene) (O) when the free-draining term is neglected and (Δ) when the free-draining contribution is taken into account; the solid line shows the behavior of a Gaussian chain of the same radius of gyration. Γ_0 is the first cumulant in the limit of $q = 0$.

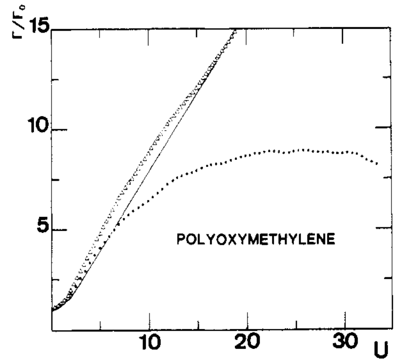

Figure 3. Normalized apparent diffusion coefficient of poly(oxymethylene) (symbols as in Figure 2).

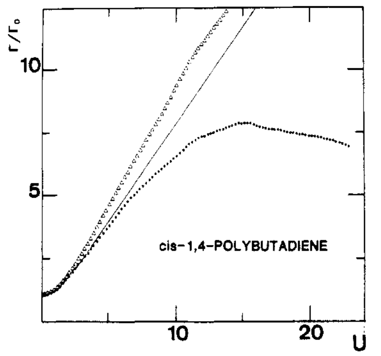

Figure 4. Normalized apparent diffusion coefficient of *cis*-1,4-polybutadiene (symbols as in Figure 2).

Edwards et al.[16] have carried out similar Monte Carlo simulations on the basis of the RIS model for the particle scattering factor of cyclic poly(dimethylsiloxanes). Their technique seems to differ, however, from that used in this paper. The apparent diffusion coefficient, D_{app}, or reduced first cumulant, $\Gamma/q^2 = D_{app}(q)$, behaves also characteristically for each polymer as is shown in Figures 2–5. The behavior at small q, i.e., $u^2 \ll 1$, and at large q may be discussed again separately.

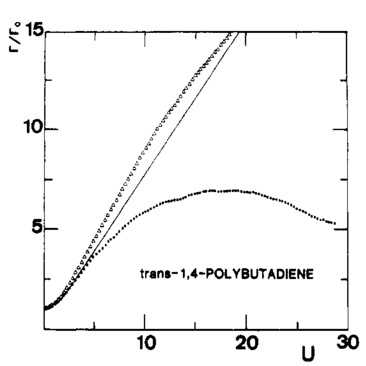

Figure 5. Normalized apparent diffusion coefficient of *trans*-1,4-polybutadiene (symbols as in Figure 2).

Table I

Coefficient C in Eq 12, Characteristic Ratio C_∞, Parameter ρ, and Value of the Asymptote Γ at Large q after Monte Carlo Simulations on the Basis of the RIS Model[a]

polymer	C	C_∞	ρ	$(\eta_0/k_BT)\cdot(\Gamma/q^3)$
cis-1,4-polybutadiene	0.1804	3.76	1.45	0.067
trans-1,4-polybutadiene	0.1851	5.80	1.46	0.070
poly(methylene)	0.1870	6.87	1.48	0.072
poly(oxymethylene)	0.2022	8.16	1.60	0.078
Gaussian chain	0.1733	1.00	1.504	0.0625
Experimental Data				
poly(dimethylsiloxane)		5.7–6.2	1.11	
poly(methyl methacrylate)		6.9	1.16	
polystyrene		10.2	1.28	

[a] For comparison the data for the Gaussian chain and some experimental results are given.

At small u^2 we should find behavior of eq 12 where the coefficient C depends on branching, chain stiffness, and polydispersity. Branching and polydispersity are excluded in these cases, but influence of the particular microstructure can be expected. Table I gives a list of the C coefficients together with the characteristic ratios C_∞, the ρ parameters, and the coefficients in the asymptotic slopes, which will be discussed below. A small but apparently significant increase of C with chain stiffness is observed. Though special details fo the different microstructures are less detectable, the ordered microstructure of poly(oxymethylene) seems to be reflected in higher ρ and C values than expected from a smooth extrapolation of the other data. The hybrid theory[10,11] exhibits no marked upturn of both ρ and C with increasing chain stiffness as observed here for poly(oxymethylene). Considering the pronounced gauche conformation in poly(oxymethylene), the higher ρ and C values than expected may be attributed to its helical sequence blocks.

In all cases the C values are larger than for the idealized Gaussian chain where $C_{Gaussian} = 0.1733$.[3] The value of C depends in the hybrid theory necessarily on the chain length for a given chain stiffness (i.e., Kuhn length) and eventually approaches 0.1733 in the limit of infinitely long chains. At finite chain length the C coefficients also increase with Kuhn length. Thus our simulation data are in qualitative agreement with this theory. Furthermore, it should be noted that the C value decreases in this hybrid theory when the minimum hydrodynamic interaction range is set larger. In Figure 6 the minimum hydrodynamic interaction range is set to 1.5 and 3 Å, respectively. To attain a better fit for C this distance should be even shorter, whereas a value of 3 Å was found reasonable to fit the simulated ρ values. This inconsistency may be due again to the different microstructures. The theoretical curves in Figure 6 were calculated in terms of C_∞ by using the relationship

$$C_\infty \sim (L/nb)(1/\lambda b) \qquad (16)$$

where L denoted the contour length given by the projection of the fully extended chain, b the bond length, and $1/\lambda$ the Kuhn length. Whether or not the numerical values of C_N remain independent of chain length has to be checked by further simulations with much longer chains. We are inclined, however, to believe that C_N for $N > 400$

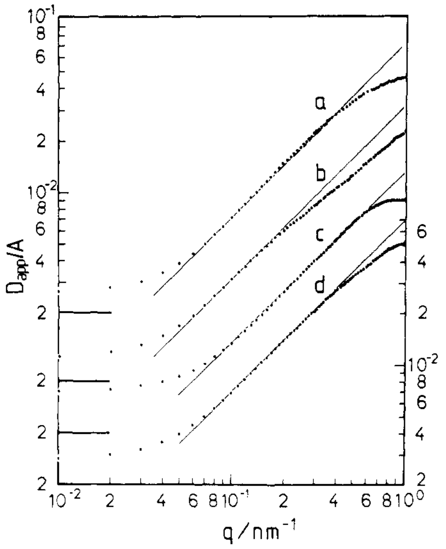

Figure 6. log–log plots of the apparent diffusion coefficients against q, where $A = k_BT/(6\pi^{3/2}\eta_0)$: (a) poly(methylene); (b) poly(oxymethylene); (c) *cis*-1,4-polybutadiene; (d) *trans*-1,4-polybutadiene. (The free draining term is taken into consideration.) Deviations from the intermediate asymptotes occur at lower q values for the stiffer chains (b) and (d).

remains indeed constant for the arguments which were presented in part 1 (no change of ρ and C_∞ when N is increased).

At large q values the predicted asymptotic behavior of Γ/q^3 = constant was not attained for any of the chosen chains when nondraining is assumed. Such behavior can be expected only as long as the free-draining contribution can be neglected, i.e., in a region of $qb < 0.1$. At larger q values, which correspond to subchain length of $N \simeq 10$, the free-draining term has already a remarkable influence. Taking into consideration the free-draining term

$$\Gamma_{\text{free draining}} = (k_BT/\zeta)(q^2/NP(q)) \tag{17}$$

we find, indeed, over a wide range the expected q^3 asymptote with values for $(\eta_0/k_BT)(\Gamma/q^3)$ as given in the last column of Table I. Here the frictional coefficient was assumed as

$$\zeta = 6\pi\eta_0(b/2) \tag{18}$$

which corresponds to $B = 0.69$ in Akcasu's notation.[12]

Our results are qualitatively in agreement with earlier calculations by Akcasu et al.,[13] who also took into account the free-draining contribution but who considered only Gaussian chains. For the more realistic chains the values for the asymptotes seem in this simulation slightly to increase with the characteristic ratio C_∞ as is shown in Table I.

With increasing chain stiffness the region of a q^3 dependence apparently becomes smaller, and deviations toward a weaker asymptotic behavior occur already at lower q values. This is shown for the poly(oxymethylene) chain in (Figure 6d). Nicholsen et al.[14] have observed a similar tendency with various polymers by quasi-elastic neutron scattering. Poly(dimethylsiloxane) as the most flexible chain shows, for instance, the expected q^3 dependence for Γ while polystyrene and poly(tetrahydrofuran) with larger persistence lengths exhibit lower exponents than 3 in their q dependences. Eventually, for very large q, in a region where $qb \gg 1$, a q^2 dependence of Γ is again observed, which reflects the local chain relaxation. The region of the transition from the q^3 dependence of a quasi-Gaussian chain to the final q^2 dependence is certainly characteristic of the local chain structure but has not sufficiently been covered by the present simulation. No general behavior can be expected and indeed is observed.

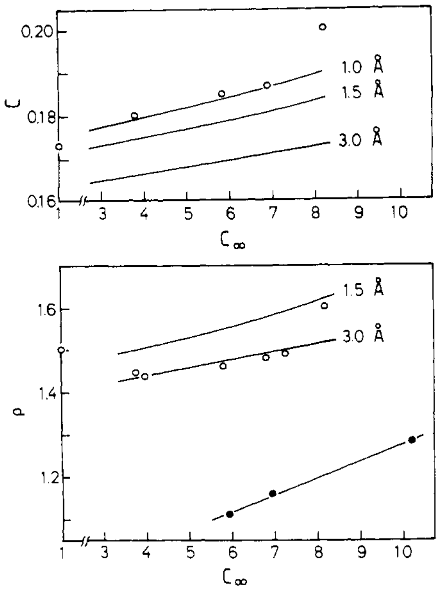

Figure 7. Dependence of the initial coefficient C in the angular dependence of the apparent diffusion coefficient on the characteristic ratio (chain stiffness) C_∞ (upper part) and the dependence of the ρ parameter on the characteristic ratio C_∞; the open circles represent the data of the computer simulation and the filled circles represent the experimentally observed data (see Table I). Curves indicated by 1.5 and 3 Å indicate the chain diameters in the hybrid theory of Koyama.

We close this discussion with two remarks. Benmouna et al.[15] predict on the basis of their sliding-rod model two intermediat subasymptotes. One corresponds to the q^3 dependence as already discussed; the second should show a $q^3 \ln (1/qb)$ behavior of a rigid rod at larger q values. We have observed no noticeable crossover to a stronger than q^3 dependence. Possibly the simulated chains are too short as to warrant the asymptotic behavior predicted by the sliding-rod model. The sliding-rod model gives, apparently,[5] a good description of the dynamic structure factor at small q.

The second remark is concerned with the coupling of translational and rotational motions. Such coupling is probably small for Gaussian chains but should not be dismissed for rigid rods. Recent calculations by Rallison and Leal[5,6] show, for instance, for the coefficient C in eq 12 a drop of $^1/_{10}$ when the coupling is neglected (Pecora) down to $^1/_{18}$ when the translation–rotation coupling is taken into account. This effect may have a significant influence on the asymptotic region of very large q and requires a modification of the present model. This modification will be treated in a forthcoming paper.

In summary, we can state the following: (i) The application of the RIS model, as the better representation of a real chain next to the Gaussian chain model, shows dependence of the ρ parameter, the coefficient C, and the coefficient in the q^3 dependence of Γ on chain stiffness. (ii) These results stand in qualitative good agreement to a recent theory by Schmidt and Stockmayer developed on the basis of the wormlike chain model.[5] (iii) The far-q region requires a modification of the present simulation to take into account the coupling between translation and rotation of the rodlike segments.

References and Notes

(1) Kajiwara, K.; Burchard, W. *Macromolecules*, preceding paper in this issue.
(2) Akcasu, A. Z.; Gurol, H. *J. Polym. Sci., Polym. Phys. Ed.* **1976**, *14*, 1.

(3) Burchard, W.; Schmidt, M.; Stockmayer, W. H. *Macromolecules* **1980**, *13*, 580.
(4) Burchard, W. *Adv. Polym. Sci.* **1983**, *48*, 1.
(5) Schmidt, M.; Stockmayer, W. H. *Macromolecules* **1984**, *17*, 509.
(6) Rallison, J. M.; Leal, L. *J. Chem. Phys.* **1981**, *74*, 4819.
(7) Flory, P. J. "Statistical Mechanics of Chain Molecules"; Interscience: New York, 1969.
(8) Zierenberg, B.; Carpenter, D. K.; Hsieh, J. H. *J. Polym. Sci., Polym. Symp.* **1976**, *No. 54*, 145.
(9) Kratky, O.; Porod, G. *Recl. Trav. Chim. Pays-Bas* **1949**, *68*, 1106.
(10) Koyama, R. *J. Phys. Soc. Jpn.* **1973**, *34*, 1029.
(11) Schmidt, M., Personal communication.
(12) Akcasu, A. Z.; Benmouna, M.; Han, C. C. *Polymer* **1980**, *21*, 866.
(13) Benmouna, M.; Akcasu, A. Z. *Macromolecules* **1980**, *13*, 409.
(14) Nicholson, L. K.; Higgins, J. S.; Hayter, J. B. *Macromolecules* **1981**, *14*, 836.
(15) Benmouna, M.; Akcasu, A. Z.; Daoud, M. *Macromolecules* **1980**, *13*, 1703.
(16) Edwards, C. J. C.; Richards, R. W.; Stepto, R. F. T.; Dodgson, K.; Higgins, J. S.; Semlyen, J. A. *Polymer* **1984**, *25*, 365.

Liquid-Crystalline Ordering in Solutions of Semiflexible Macromolecules with Rotational-Isomeric Flexibility

Alexei R. Khokhlov* and Alexander N. Semenov

Physics Department, Moscow State University, Moscow 117234, USSR.
Received December 28, 1983

ABSTRACT: The orientational ordering in solutions of semiflexible macromolecules with rotational-isomeric flexibility is considered. It is shown that in this case the liquid-crystalline transition has many features essentially different from the corresponding features for persistence or freely jointed flexibility models: the isotropic phase becomes unstable at lower polymer concentrations and the appearing anisotropic phase is much more ordered and more concentrated; the width of the phase separation region is thus anomalously large. The transition properties depend essentially on the ratio of two flexibility parameters: the length of the usual Kuhn segment of the chain controlled by the rotational isomerism and the length of a *second* Kuhn segment (concept introduced in this paper) connected with a small persistent flexibility component, which is always present in real chains. The behavior of a solution of semiflexible rotational-isomeric chains in external orientational fields of dipole and quadrupole types is analyzed as well. It is shown that to suppress the phase transition, which takes place when the solution is concentrated, it is necessary to apply much stronger fields than for the persistence or freely jointed flexibility models. A phase transition can be induced by an external orientational field at practically any concentration of the initially isotropic solution. The susceptibility of the solution in zero dipole field, χ_0, in the case under consideration increases with the solution concentration in the anisotropic phase, c, according to the power law $\chi_0 \sim c^{5/2}$ (to be compared with the exponential increase for the persistence model and with practical independence of c for the freely jointed model).

1. Introduction

It is well-known that in sufficiently concentrated solutions of stiff-chain polymers an orientationally ordered phase can appear. In ref 1–5 the corresponding liquid-crystalline phase transition was studied in detail for the case of completely stiff macromolecules (long, absolutely rigid rods). Accounting for the partial flexibility of the chain of a stiff polymer naturally constitutes the next fundamental problem. This problem has been considered in recent papers by Flory and Matheson[6,7] and by Ronca and Yoon,[22-24] and in our papers.[8-11] From the theoretical point of view the simplest partially flexible chains are the so-called semiflexible macromolecules whose effective Kuhn segment length, l, is much smaller than the total contour chain length, L, but much larger then the width of the chain, d: $L \gg l \gg d$. The consideration of a solution of chains for which $L \sim l$ is much more complex.[11]

Semiflexible macromolecules can differ depending on the flexibility mechanism of a polymer chain. Simplest is the freely jointed model, where the chain can be represented as a sequence of freely jointed rigid rods of length l and diameter d (Figure 1). Orientational ordering in solutions of semiflexible freely jointed macromolecules was considered in 1978 independently in ref 6 and 8. It was shown that the properties of the liquid-crystalline transition are practically the same as in a solution of disconnected rigid rods of length l and diameter d.

It should be emphasized, however, that freely jointed chains are encountered very rarely in the real polymer world. The most common flexibility models are the persistence one (which is due to the gradual accumulation of the effect of small thermal vibrations of valence angles, bonds, etc.) and the rotational-isomeric one.[12] Persistent semiflexible chains can be represented as long, absolutely homogeneous elastic filaments of width d and a Kuhn segment length l (Figure 2). The liquid-crystalline transition in a solution of semiflexible persistent chains was considered in ref 10; it was shown that it takes place at significantly higher polymer concentrations and that the order parameter at the transition point is much smaller than for a solution of freely jointed chains with the same parameters d and l. Thus, the results of ref 10 permit us to conclude that the conditions for orientational ordering in solutions of semiflexible polymers depend in an essential way on the mechanism of the chain flexibility.

It is consequently important to analyze the liquid-crystalline transition in solutions of semiflexible chains with other flexibility models (differing from the freely jointed and persistence ones) and, primarily, with the widely used rotational-isomeric flexibility model. This is precisely the aim of the present paper.

It is noteworthy that the majority of known polymers able to form a liquid-crystalline phase in solution (helical polypeptides, aromatic polyamides[13]) exhibit a persistence flexibility mechanism. At the same time, there is no fundamental reason why liquid-crystalline solutions of rotational-isomeric semiflexible macromolecules should not exist. Taking into account the recent intensive increase of the number of papers on the synthesis of new classes of stiff-chain polymers[14] and the prevalence of the rota-

0024-9297/84/2217-2678$01.50/0